RADIOCARBON, Vol 55, Nr 1, 2013, p 115–126 © 2013 by the Arizona Board of Regents on behalf of the University of Arizona

IMPROVING ANTARCTIC SEDIMENT ^{14}C DATING USING RAMPED PYROLYSIS: AN EXAMPLE FROM THE HUGO ISLAND TROUGH

Brad E Rosenheim[1] • Jennifer A Santoro[2,3] • Madeleine Gunter[2,4] • Eugene W Domack[2]

ABSTRACT. To improve the chronology of sediments containing information about Holocene ice shelf and oceanic dynamics in the vicinity of the Antarctic Peninsula, we compare bulk acid-insoluble radiocarbon dating to ramped pyrolysis ^{14}C dating in a sediment core containing ample organic material. This core spans the last 12,000 yr of open-shelf sedimentation in the Bellingshausen Sea, western Antarctic Peninsula. By estimating the spectrum of ^{14}C ages within a given core horizon, the ramped pyrolysis ^{14}C method separates organic carbon relative to thermal stability, isolating younger parts of the mixture from older ones and providing an estimate of the geological uncertainty inherent in a bulk ^{14}C age. Employing the ramped pyrolysis ^{14}C method to this core demonstrates variable bulk ^{14}C age bias and increasing age spectrum downcore, neither of which can be associated with major changes in lithology of the core. The chronology of the sediment core using the youngest ages from the ramped pyrolysis technique allows for correlation between nearby Palmer Deep sediments and these sediments from the Hugo Island Trough.

INTRODUCTION

Sediment cores have been widely studied for records of the Earth's history, and recent emphasis on climate comparisons has necessitated improved chronology for correlation of global and regional events. This has posed challenges in some sedimentary environments. The high latitudes, for example, are sensitive to climate change and thought to be regions that drive and/or amplify global climate feedbacks. Antarctica, containing the largest amount of continental ice, is increasingly important in relating past climate changes to anthropogenic climate change because of its potential to cause meter-scale sea-level rise in addition to the information on past climate records preserved in its ice cores (Andrews et al. 1999). The Southern Ocean is also a site of high primary productivity and, regionally, high sedimentation rates. Potentially high-resolution sediment cores in Antarctica have offered opportunities for correlation of sedimentary facies changes to global climate events such as those recorded in nearby high-resolution ice cores. However, this objective is generally rendered difficult due to the lack of preserved, datable calcium carbonate that would provide the chronological foundation for such correlations in sediment cores that have not been perturbed by infauna or ice.

In past studies, bulk radiocarbon dating of the acid-insoluble organic matter (AIOM) has been the most popular chronology method (DeMaster et al. 1996; Licht et al. 1998; Domack et al. 2001), but it is difficult to prove the chronological relevance of the AIOM to sediment deposition. The sources of carbon in AIOM are potentially representative of many different pathways to the sedimentary depositional environment; as such, the measurement of the AIOM ^{14}C age yields an average age for these sources. In general, the majority of these different sources are older than the carbon recently fixed by primary producers at the time of sediment deposition. Therefore, AIOM ages are generally contaminated with carbon older than the time of deposition. Most researchers have assumed that these proportions would be constant through the age of the core, and therefore using core-top ages have been widely used for downcore age correction in Antarctic and other sediment chronology (Pudsey et al. 1994; Licht et al. 1998; Andrews et al. 1999; Domack et al. 2001; Mosola and Anderson 2006; Michalchuk et al. 2009). This paradigm has been followed despite evidence that significant changes in organic matter do happen downcore (Domack et al. 1993, 1995; Shevenell et al. 1996; Rosenheim et al. 2008; Michalchuk et al. 2009; Milliken et al. 2009).

[1]Department of Earth and Environmental Sciences, Tulane University, New Orleans, Louisiana, USA. Corresponding author. Email: brosenhe@tulane.edu.
[2]Department of Geosciences, Hamilton College, Clinton, New York, USA.
[3]Presently at Nicholas School of the Environment, Duke University, Durham, North Carolina, USA.
[4]Presently at Department of Anthropology, College of William and Mary, Williamsburg, Virginia, USA.

https://doi.org/10.2458/azu_js_rc.v55i1.16234 Published online by Cambridge University Press

Ramped pyrolysis (RP) ^{14}C analysis has been employed as an alternative for bulk AIOM dating for sediments where carbonate minerals are not preserved well enough for age models (Rosenheim et al. 2008). This method allows increasing temperature to thermally break down organic carbon (OC) at a rate of (5 K min^{-1}): slow enough to allow separation of more thermochemically reactive constituents from more diagenetically stable ones. The method differs from previous applications of pyrolysis and variable temperature combustion in ^{14}C applications (McGeehin et al. 2001, 2004; Wang et al. 2003) in that the temperature trend is smooth, not stepped, and therefore assumes nothing about the temperatures at which certain OC constituents would be expected to volatilize. The method has been shown to improve AIOM ^{14}C ages by up to 10,000 ^{14}C yr (Rosenheim et al. 2008) when applied at high resolution (>3 ^{14}C measurements per sediment horizon) to sediment that was contaminated with aged carbon at the time of deposition. Additionally, RP ^{14}C analysis allows verification of constant mixing ratio assumptions of pre-aged OC into the core sediment.

Despite the success in improving AIOM ages, sequential downcore dates at high resolution have not yet been analyzed for a single sediment core. Here, we apply RP ^{14}C analysis to a kasten core (KC-11) from the Hugo Island Trough in the Palmer Deep region of western Antarctic (Figure 1) that spans the Holocene period, and we compare the RP ages directly to bulk AIOM ages and to the nearby Palmer Deep ^{14}C chronology via magnetic stratigraphy (Domack et al. 2001). This detailed investigation into the application of RP ^{14}C analysis to a sediment core with consistent lithology provides a formidable test for the constant mixing ratio hypothesis routinely employed in Antarctic sediment chronology. This offers a potential improvement to sediment chronology in Antarctica in addition to necessary changes in reservoir age through time (van Beek et al. 2002).

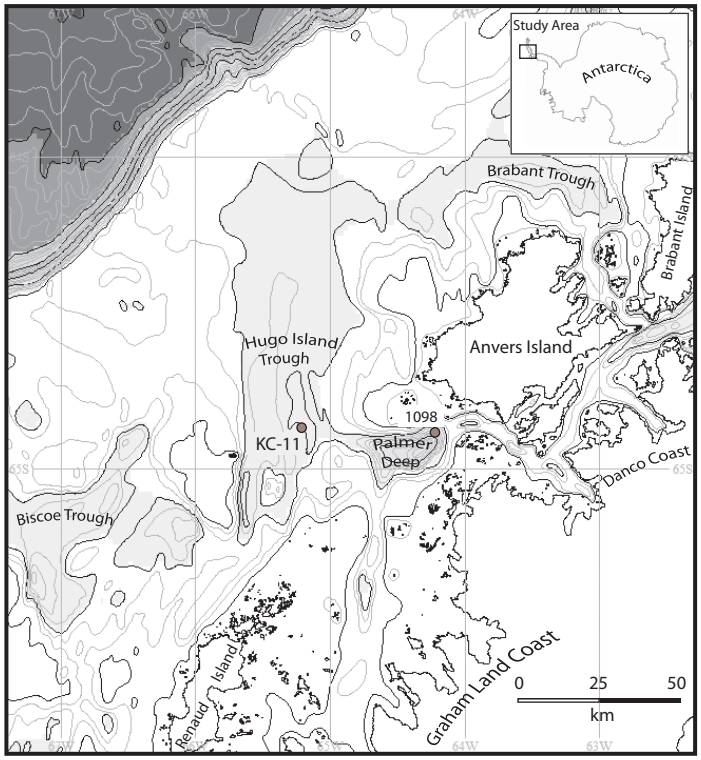


Figure 1 Location of core KC 11 on the west coast of the Antarctic Peninsula (contour interval = 250 m). Inset shows location relative to the continent of Antarctica.

https://doi.org/10.2458/azu_js_rc.v55i1.16234 Published online by Cambridge University Press

The region of the Palmer Deep and the Hugo Island Trough is important in addressing the timing of the deglaciation of the Antarctica Peninsula, a point recently underscored by the difference in the Palmer Deep record of deglaciation and chronologies from several different ice streams further seaward on the shelf (Mackintosh et al. 2011; Weber et al. 2011). Thus, this manuscript represents an important advance to establishing an accurate and potentially diachronous timing of deglaciation in Antarctica using a more detailed chronology along the same ice stream as the Palmer Deep.

METHODS

Sediments were collected from the *Nathaniel B Palmer* (NBP 10-01) in the Hugo Island Trough (64°50.902′S, 65°23.982′W) at a depth of 636 m on the open shelf (KC-11, Figure 1). A previous core from the nearby Palmer Deep (Domack et al. 2001, 2006) showed a polynomial age model based on 78 acid-insoluble organic matter (AIOM) and foraminifera ^{14}C chronologies and stands as the best-resolved Holocene marine chronology in the Southern Ocean (Figure 2). Our results will therefore be comparable to the Palmer Deep due to the proximity of these 2 cores (Domack et al. 2005).

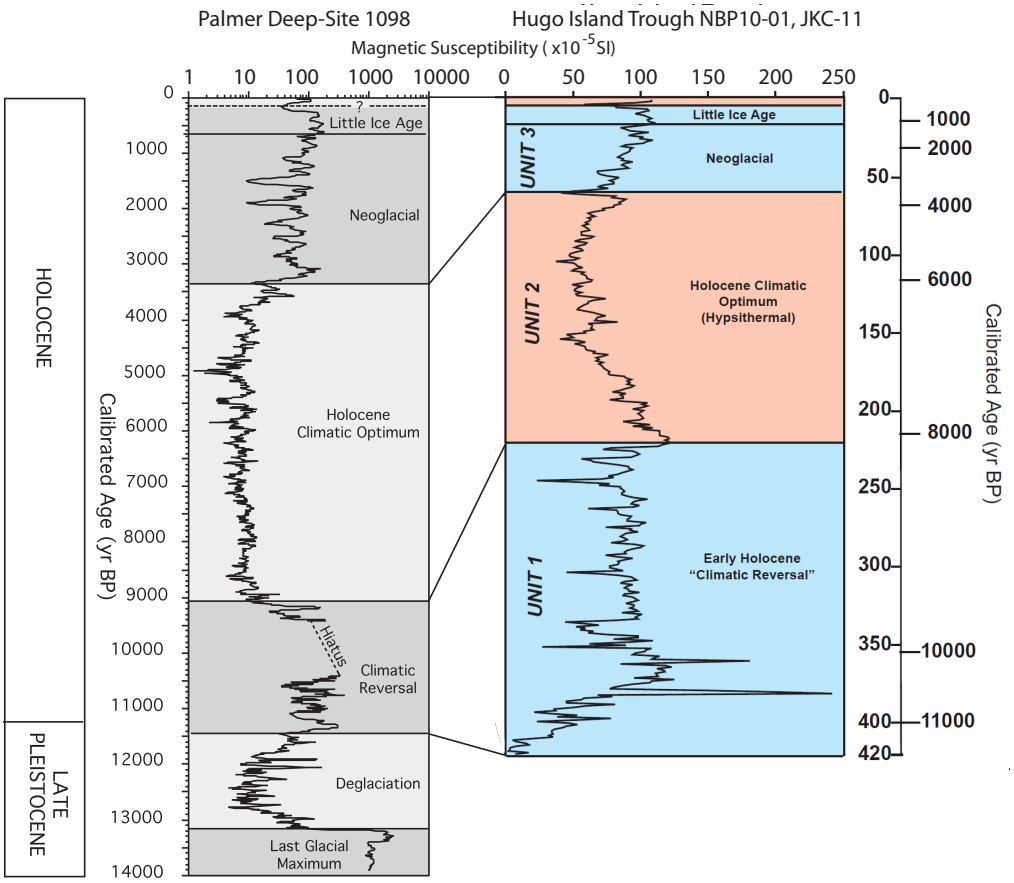


Figure 2 Comparison of magnetic susceptibility in Palmer Deep sediment dated by 78 radiocarbon dates and Hugo Island Trough sediment dated by ramped pyrolysis ^{14}C dating. Major trends in the 2 records match in time based on the chronologies, including low magnetic susceptibility in the mid-Holocene and raised magnetic susceptibility in the early Holocene deglaciation of this area.

https://doi.org/10.2458/azu_js_rc.v55i1.16234 Published online by Cambridge University Press

The Hugo Island Trough core (NBP 01-10 KC-11) was sampled at 5 separate depth intervals (Table 1) and then immediately dried shipboard at 40 °C for 24–48 hr to minimize the potential for chemical alteration of organic matter during shipment and transfer. At the Stable Isotope Laboratory at Tulane University (SILT U), the samples were pulverized to uniform consistency and treated with 2N HCl for 24 hr to dissolve carbonate minerals. All samples were then centrifuged for 2 min until the sediment settled, and decanted. They were subsequently rinsed with laboratory-filtered water (18.2S resistivity), centrifuged, and decanted in a series of repeated steps until the pH of the supernatant approached 7. Samples were then dried in individual precombusted (525 °C, 2.5 hr) aluminum pans at 60 °C for 65 hr. Dried samples were stored in precombusted (525 °C, 2.5 hr) vials until analysis.

Table 1 Summary of acid-insoluble organic matter (AIOM) including age determinations, $\delta^{13}C$ and fraction modern (Fm) for the NBP 10-01 KC-11 core (NOSAMS Facility, WHOI). Values of $\delta^{13}C$ are reported relative to PDB.

Core depth (cm)	Sample	Max temp of interval (°C)	CO_2 evolved (mol)	Fm (1σ)	Age (yr)	Age ± error	$\delta^{13}C$ (1σ)
0–1	Measured AIOM			0.7667 (0.0034)	2130	35	–24.9 (0.1)
	DB-42-1	326	27.899	0.7907 (0.0019)	1890	20	–26.4 (0.1)
	DB-42-2	403	30.420	0.7773 (0.0017)	2020	15	–25.9 (0.1)
	DB-42-3	465	30.420	0.7678 (0.0017)	2120	20	–25.6 (0.1)
	DB-42-4	547	31.092	0.7573 (0.0035)	2230	35	–27.0 (0.1)
	DB-42-5	847	22.525	0.6939 (0.0044)	2930	50	–26.7 (0.1)
100–101	Measured AIOM			0.4333 (0.0029)	6720	55	–24.1 (0.1)
	DB-43-1	345	29.119	0.4475 (0.0014)	6460	25	–25.5 (0.1)
	DB-43-2	421	38.498	0.4441 (0.0027)	6520	50	–25.7 (0.1)
	DB-43-3	479	33.421	0.4422 (0.0026)	6550	45	–25.2 (0.1)
	DB-43-4	559	29.892	0.4325 (0.0035)	6730	65	–25.7 (0.1)
	DB-43-5	915	21.983	0.4045 (0.0024)	7270	45	–24.9 (0.1)
200–201	Measured AIOM			0.3127 (0.0036)	9340	90	–24.5 (0.1)
	DB-45-1	351	29.926	0.3335 (0.0024)	8820	60	–26.0 (0.1)
	DB-45-2	430	34.471	0.3222 (0.0022)	9100	55	–26.3 (0.1)
	DB-45-3	497	29.307	0.3180 (0.0017)	9200	40	–25.1 (0.1)
	DB-45-4	582	29.798	0.3077 (0.0015)	9470	40	–25.5 (0.1)
	DB-45-5	948	16.625	0.2795 (0.0029)	10,250	80	–25.0 (0.1)
300–301	Measured AIOM			0.2553 (0.0036)	10,950	110	–24.2 (0.1)
	DB-62-1	358	30.612	0.2865 (0.0024)	10,050	65	–26.0 (0.1)
	DB-62-2	436	36.578	0.2839 (0.0023)	10,100	65	–18.8 (0.1)
	DB-62-3	497	29.341	0.2870 (0.0033)	10,050	95	–8.9 (0.1)
	DB-62-4	566	28.939	0.2657 (0.0012)	10,650	35	–25.3 (0.1)
	DB-62-5	946	26.849	0.2195 (0.0036)	12,200	130	–28.0 (0.1)
398–399	Measured AIOM			0.2145 (0.0047)	12,350	170	–24.7 (0.1)
	DB-50-1	363	33.767	0.2518 (0.0020)	11,100	65	–26.6 (0.1)
	DB-50-2	444	41.413	0.2418 (0.0037)	11,400	120	–26.5 (0.1)
	DB-50-3	510	30.390	0.2158 (0.0015)	12,300	55	–25.1 (0.1)
	DB-50-4	589	29.670	0.2060 (0.0014)	12,700	55	–25.6 (0.1)
	DB-50-5	921	19.482	0.1613 (0.0025)	14,650	120	–25.4 (0.1)

Small aliquots (5–10 mg) of each acidified and dried sample were analyzed in an Elementar Vario MicroCube elemental analyzer (EA) by enclosing the samples in tin capsules and flash-combusting them at 950 °C to determine the %TOC of the samples. Larger aliquots of ~100–300 mg of dried sediment were placed in a precombusted (900 °C, 4.5 hr) quartz reactor tube between plugs of precombusted (900 °C, 4.5 hr) quartz wool. Samples were analyzed in the same fashion as previous RP ^{14}C analyses of Antarctic sediments (Rosenheim et al. 2008): briefly, with a temperature ramp of

https://doi.org/10.2458/azu_js_rc.v55i1.16234 Published online by Cambridge University Press

5 K min^{-1}, ~8% O_2 joining the volatiles after the pyrolysis furnace, and flowing through a Sable Systems Ca-10 infrared gas analyzer calibrated to measure CO_2. Sample CO_2 gas was collected at 5 intervals of approximately 20–30 μmol (Table 1), cryogenically separated from other condensable and non-condensible gases using a series of liquid nitrogen (–195 °C) and liquid nitrogen-cooled isopropanol (–70 °C) traps, and sealed into evacuated 6-mm Pyrex® tubes with precombusted (525 °C, 2.5 hr) copper oxide and granulated silver. Sample intervals were determined based on sample size and therefore not taken at exactly the same intervals for every sample. The tubes were recombusted at 525 °C for 2.5 hr to remove any possible sulfur compounds prior to graphitization.

At the National Ocean Sciences Accelerator Mass Spectrometry Facility (NOSAMS) at the Woods Hole Oceanographic Institution, samples of demineralized sediments were loaded into quartz tubes with precombusted (525 °C, 5 hr) copper oxide and silver granules, sealed, and heated to 900 °C for 6 hr to generate bulk AIOM CO_2 from each sample analyzed by ramped pyrolysis. About 10% of each CO_2 sample, including both the bulk samples and the ramped pyrolysis samples, was used to determine $\delta^{13}C$ ratios. The remainder of each CO_2 sample was graphitized by conventional Fe-H_2 reduction techniques, packed into aluminum targets, and ionized using a Cs^+ sputter ion source for determination of $^{14}C/^{12}C$ ratios by AMS (Table 1).

RESULTS

Overall, each of the 5 samples needed to be heated to 950 °C in order to completely volatilize all of the carbon into CO_2 (Table 1, Figure 2). Yields calculated from RP ^{14}C analysis were quantitative (average 99.6 ± 3.7% using EA analysis as true value, Figure 3). Measured bulk ages and stable carbon isotope values are compared with calculated bulk values of the same parameters from ramped pyrolysis analysis (Table 1), where the calculated bulk isotope values ($\delta^n C_{cb}$) can be expressed as:

$$\delta^n C_{cb} = \sum_{i=1}^{k} f_i \times \delta^n C_{ci} \quad (1)$$

where n is the isotope (13 or 14), f_i is the proportion of each ramped pyrolysis temperature interval's CO_2 aliquot to the total CO_2 evolved by the reaction, k is the number of measured temperature intervals, and $\delta^n C_i$ is each individual measured isotope (^{13}C or ^{14}C) ratio. We assume that $\delta^{14}C \approx \Delta^{14}C$ (Stuiver and Polach 1977) due to the short time between sample collection and analysis (maximum 2 yr), and this quantity is related to calculated bulk fraction modern and age in the same way as measured values (Stuiver and Polach 1977). Values of $\delta^{14}C_{cb}$ are indistinguishable from measured bulk $\Delta^{14}C$ (Figure 4, Table 1), but values of $\delta^{13}C_{cb}$ are displaced from the 1:1 line by nearly 1‰ PDB, with the exception of 1 point that incorporates very high $\delta^{13}C$ values (Figure 4, Table 1). In all cases, this did not affect the ^{14}C determinations because of corrections for fractionation (Stuiver and Polach 1977) and preservation of ^{14}C mass balance (Figure 4).

Bulk ^{14}C ages (and calculated bulk ages) increase downcore as expected from the sediment facies sampled by this core. Ages of the low-temperature ramped pyrolysis (RP) samples also increase downcore. However, the rate at which they increase differs from the rate measured from bulk ages (Figure 5). In addition, all low-temperature RP ^{14}C ages are younger than their correlative bulk ages. For example, the difference in age between low-temperature RP intervals and bulk samples increases from 240 ^{14}C yr at 0–1 cm to 1250 ^{14}C yr at 398–399 cm (Figure 5).

https://doi.org/10.2458/azu_js_rc.v55i1.16234 Published online by Cambridge University Press

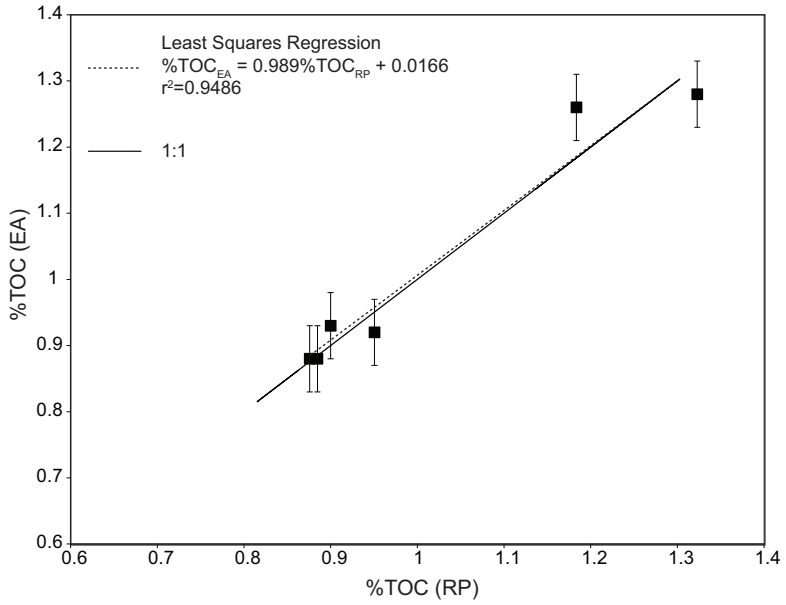


Figure 3 Carbon content of sediment samples measured using an elemental analyzer (EA, *y* axis) and using quantification of all of the gas from a ramped pyrolysis run (RP, *x* axis). All results but one are within analytical uncertainty of the 1:1 line that represents absolute quantitative yield from the ramped pyrolysis system; regression of the data into a linear model is nearly identical to the 1:1 line.

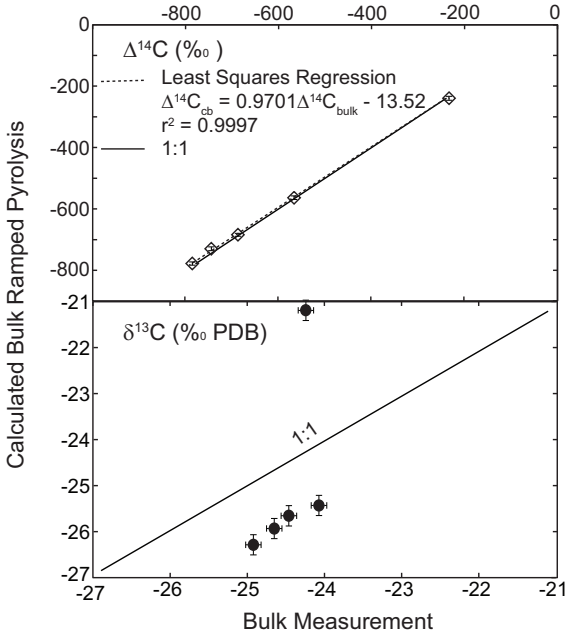


Figure 4 Calculated bulk $\Delta^{14}C$ (top) and $\delta^{13}C$ (bottom) for each sample is compared to bulk measurements of the same quantity. For ^{14}C, the values are indistinguishable, indicating that the mass balance of trapped CO_2 during ramped pyrolysis was adequate in recuperating sample without biasing ages. Least-squares regression through the data is indistinguishable from the 1:1 line. Stable carbon isotopes, on the other hand, indicate fractionation. This does not affect ^{14}C values because of isotope corrections.

https://doi.org/10.2458/azu_js_rc.v55i1.16234 Published online by Cambridge University Press

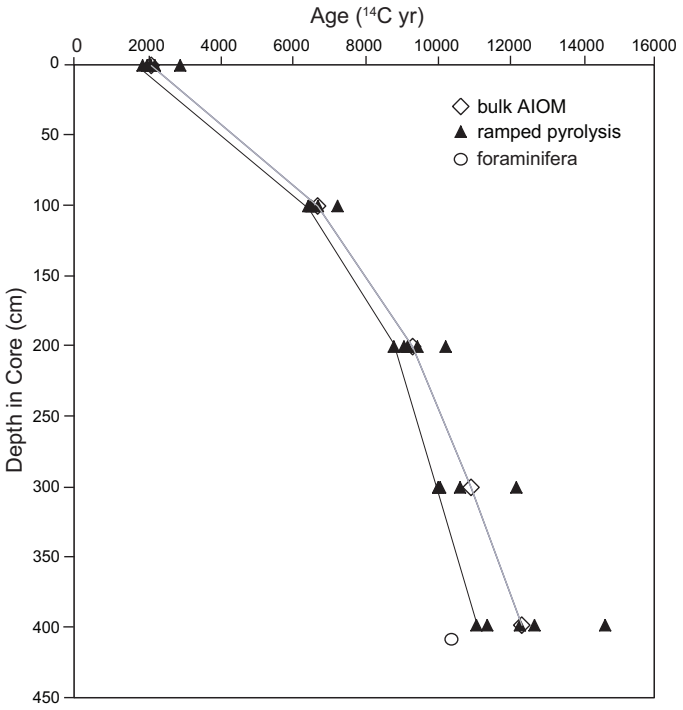


Figure 5 Bulk ^{14}C ages and those of the low-temperature fraction of ramped pyrolysis (RP) both increase going downcore. RP ages increase more slowly downcore indicating increasing proportion of pre-aged C downcore. This is supported by larger age spectra downcore. Most importantly, low-temperature RP ages closely approach a lone foraminifera age (open circle); however, none were measured from exactly the same core horizon due to low carbonate preservation in the sediment.

DISCUSSION

Ramped pyrolysis ages from the lowest temperature interval are a significant improvement in the accuracy of age models that depend on AIOM. The data in Figure 5 show that the age model can be made more accurate with ramped pyrolysis dates from the lowest-temperature fraction by up to 1250 ^{14}C yr. Calibrated age improvements using this magnitude of change could be even more significant than this, magnified up to over 4000 calendar yr during steeper areas of the calibration curve. This improvement arises from the ability of the technique to remove and analyze the more reactive carbon, which is generally younger, from the pre-aged autochthonous carbon. These ages of the lowest-temperature fraction represent maximum ages of the sediment. In the absence of similar ages at adjacent temperature intervals (age plateaus), we cannot assign these ages as the absolute age of the sediment (Figure 7). Foraminifera data, if taken as the preferred age of the sediment, suggest that absence of age plateaus may reflect a persistent overestimation of ages, underscoring the fact that these are maximum age constraints (Rosenheim et al. 2008; Figure 5 herein).

Differences between bulk AIOM dates and low-temperature pyrolysis dates are not constant, increasing from 240 to 1250 ^{14}C yr downcore (Figure 5). This indicates a change in the proportions of pre-aged organic matter downcore. We can use the ramped pyrolysis data to constrain the changes in admixed organic material, if we assume that each bulk age (measured fraction modern for the bulk AIOM) is comprised of 2 end-members:

https://doi.org/10.2458/azu_js_rc.v55i1.16234 Published online by Cambridge University Press

$$\Delta_{bulk} = \Delta_{actual}(1 - f_{pre-aged}) + \Delta_{pre-aged}(f_{pre-aged}) \quad (2)$$

where actual $\Delta^{14}C$ can be approximated by the lowest-temperature ramped pyrolysis age and the pre-aged end-member $\Delta^{14}C$ can range between –1000 (oldest possible) and the oldest measured age in this data set (youngest likely pre-aged end-member, 14,650 ^{14}C yr, Table 1), we can calculate the fraction of pre-aged carbon present:

$$f_{pre-aged} = \frac{\Delta_{bulk} - \Delta_{actual}}{\Delta_{pre-aged} - \Delta_{actual}} \quad (3)$$

This shows a large range of possible proportions of pre-aged carbon (Figure 6) that can change considerably downcore. Moreover, no matter the end-member $\Delta^{14}C$ value, the fraction increases by 5–8 times from the core top to the deepest dated horizon. It is important to note that the proportions in Figure 5 assume constant age of the pre-aged carbon end-member; any change through time in the age of the pre-aged carbon will cause variations in the nearly linear increases in these proportions, but those variations will stay between the scenarios presented in Figure 6.

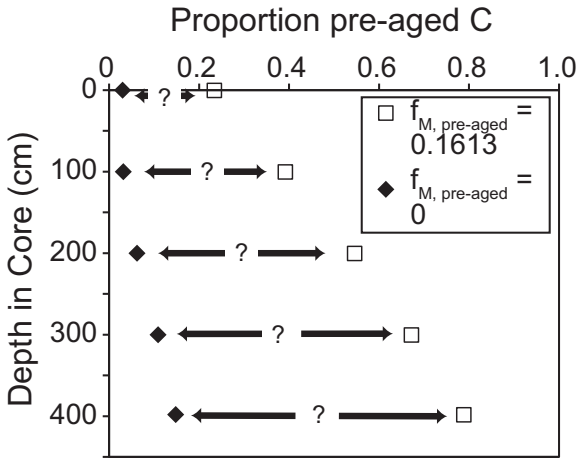


Figure 6 Downcore changes in the proportion of pre-aged carbon ($f_{pre\text{-}aged}$) using 2 different end-member ages. These values represent extremes, calculated by assuming both maximum age for the pre-aged carbon (filled diamonds) or using the maximum age of measured ramped pyrolysis intervals as the assumed pre-aged carbon (open squares). This shows that at the core top the fraction of pre-aged carbon can range from 3–23% of the TOC, whereas at the 398–399 cm interval this range increases to 15–79%. Ranges at each sediment horizon are depicted by arrows, and the question mark indicates that these constraints do not allow exact analysis of the specific fraction—such values can change in any direction between the constraints downcore.

Thermographs for each samples showed strong similarities downcore (Figure 7). The average T_{max} was 443 ± 8.6 °C, showing that there was little change between any of the samples' overall thermochemical stability. This can be attributed to the fact that the core has a largely uniform lithology, likely relating to constant sources of OC associated with the sediment. Furthermore, the overall shapes of the thermographs changed minimally downcore (Figure 7). Differences in stability of the OC of this core are evident in subtle, systematic changes to the shapes of the pyrolysis reactions (Figure 7, data normalized for relative comparison). Moving downcore, a low-temperature inflection in the pyrolysis reaction loses relative predominance to a high-temperature shoulder. Figure 7

https://doi.org/10.2458/azu_js_rc.v55i1.16234 Published online by Cambridge University Press

depicts normalized data where the areas under the curves are equal; therefore, these shifts do not necessarily relate to a change in the mass of OC of different stabilities. Rather, the data represent changes in the relative contributions of components of OC. In other words, increasing prominence of the high-temperature shoulder downcore could be due to either addition of more diagenetically stable material, loss of reactive material, or a combination of both. From a diagenetic standpoint, loss of reactive material is more likely in a stable depositional environment without much temporal change in the addition of older terrigenous material or older marine material from slope instability.

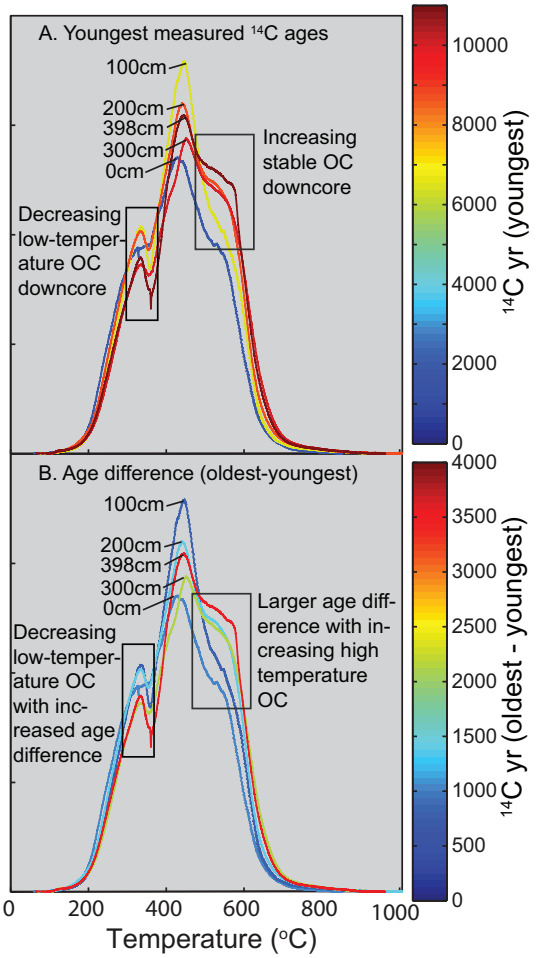


Figure 7 A) Plot of normalized (unitless) CO_2 evolution data from each of the 5 horizons analyzed by ramped pyrolysis. Each CO_2 trace is color coded with the age (^{14}C yr) of the youngest measured temperature interval. Downcore, less relatively reactive low-temperature OC is observed and the high-temperature reaction shoulder becomes more predominant. B) Same data as A, plotted with colors indicating difference between oldest and youngest measured temperature interval. Here, downcore samples have large age differences, or wider age spectra. The age difference also relates to alteration of the stability of OC to withstand higher temperatures downcore. The general trend in both panels is that age spectra shift to older ages and become wider downcore; corresponding to subtle changes in reaction shape. That the reactions do not show a wholesale shift toward higher temperatures despite an age range through the Holocene reflects the constancy of the sediment facies making up this core.

Thus, it is notable that as more reactive material is diagenetically altered and potentially lost to dissolution in porewaters, age differences increase (Figure 7b). Diagenetic alteration (i.e. condensation-type reactions) of young OC would result in stabilizing younger OC with high-temperature portions of a pyrolysis reaction, effectively narrowing the age spectrum. Differential diagenetic loss of OC to dissolution in porewaters (remineralization) would result in the observed patterns if a greater proportion of material were lost from the more reactive (low-temperature) portions of the thermograph. We interpret this to represent differential diagenetic remineralization and loss, rather than diagenetic alteration without loss of younger material within the core.

https://doi.org/10.2458/azu_js_rc.v55i1.16234 Published online by Cambridge University Press

The fact that thermographs do not significantly change shape downcore supports previous work on Antarctic sediment that illustrated the robustness of Gaussian estimations of major OC components (Rosenheim et al. 2008). In these sediments, changes in thermograph shape downcore are less pronounced than those from the Erebus and Terror Gulf (Rosenheim et al. 2008). Figure 8 shows the Gaussian decomposition of the 0–1 cm interval of the core. Using a least-squares regression to find the best fit of 3 Gaussians for the rest of the intervals yields very similar models in terms of temperatures of the centers of the Gaussians (Table 2). The shift toward more stable OC downcore (Figure 7) is verified in comparing the proportions of CO_2 assigned to each of the Gaussian components (Table 2) as there are slight increases in the proportions of G3 that coincide with decreases in the proportion of G1 downcore.

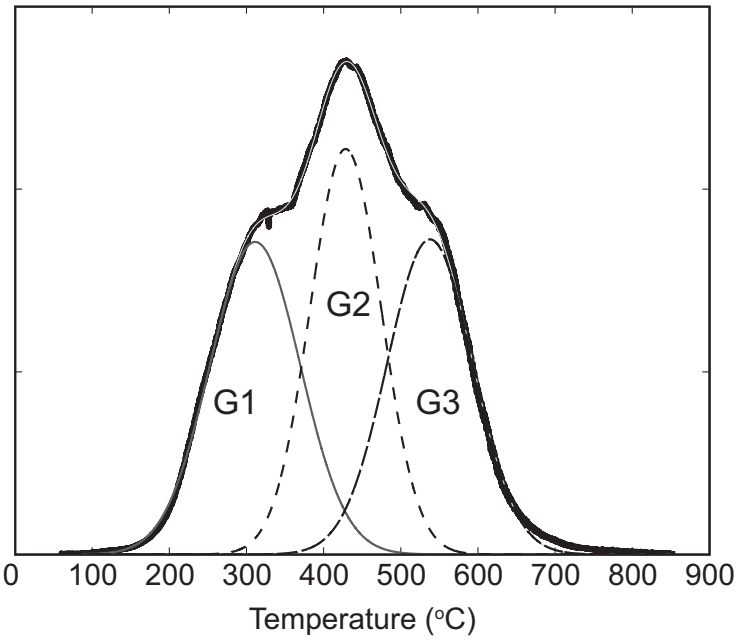


Figure 8 Gaussian decomposition of 0–1 cm interval of KC-11 core. Three Guassian curves adequately explain the thermographs for each of the sediment horizons analyzed. A thin gray line showing the sum of the Gaussians is shown, but is difficult to tell apart from the heavy line depicting the data. Center temperatures (T_{max}) and proportions of CO_2 associated with each component of each dated sediment horizon are shown in Table 2. Values of T_{max} show little change downcore (Figure 7, Table 2).

Table 2 Center temperatures (in °C) and proportions of Gaussians used to model the 3 dated depth horizons in KC-11. Models of 3 Gaussians were adequate for all horizons.

Core depth (cm)	G1 Temp	G1 proportion	G2 Temp	G2 proportion	G3 Temp	G3 proportion
0–1	311	32.64	428	34.16	537	33.2
100–101	323	31.2	439	37.16	546	31.63
200–201	325	32.7	436	28.36	543	38.94
300–301	326	28.92	442	29.41	551	41.67
398–399	319	27.66	435	28.91	544	43.43

https://doi.org/10.2458/azu_js_rc.v55i1.16234 Published online by Cambridge University Press

Ultimately, understanding the chronology of these sediments is the goal of our approach. In order to assess this goal, we compare the chronology of the Hugo Island Trough sediments to the well-established chronology of sediments from the nearby Palmer Deep (Figure 1). The latter chronology consists of 78 ^{14}C dates, 8 of which came from foraminifera and the rest of which were from bulk organic acid-insoluble material, and has been useful for several recent paleoclimate studies (Mackintosh et al. 2011; Shevenell et al. 2011). Although ramped pyrolysis dates from this core reflect age maxima due to the lack of age plateaus at the low-temperature end of the spectrum, the correlation between these 2 cores suggest that these ages are close to the preferred ages of the sediment (Figure 2). As such, the ramped pyrolysis ^{14}C chronology of the Hugo Island Trough core provides an acceptable chronology while illustrating the variable nature of age offsets that are often observed in bulk organic chronologies.

CONCLUSIONS

Ramped pyrolysis ^{14}C dating of AIOM in a sediment core improves bulk organic acid-insoluble material (AIOM) ages. Comparison to the Palmer Deep chronology establishes the Hugo Island Trough ramped pyrolysis dates, indicative of age maxima in the absence of low-temperature age plateaus, as viable dates for a dependable chronology. Calculated bulk ages are indistinguishable from the measured bulk AIOM ages for each interval studied herein, demonstrating that the ramped pyrolysis method analyzes all of the organic carbon in a sample. As such, at the very least, the distribution of ramped pyrolysis ^{14}C ages represents the "geologic" uncertainty of a bulk AIOM date because it provides an estimate of the spread of ages of individual components of the whole OC pool.

Analysis of the shape of thermographs from the methods provides information about the diagenetic history of the OC in the sediment core. Whereas T_{max} changes very little from sample to sample, subtle but systematic changes in the shapes of individual thermographs are indicative of a shift to higher degrees of thermochemical stability downcore. This is corroborated by Gaussian decomposition modeling of the thermographs. This facet of our work indicates that improved chemical modeling of the pyrolysis process is a worthy goal to increase the likelihood of using this method for absolute ages of sediment where no foraminifera are present.

ACKNOWLEDGMENTS

We thank the NSF for support for this work: grant NSF-EAR-0929752 to BER (Tulane University) and NSF-OPP-ANT-0732467 to EWD (Hamilton College) funded instrumental development and sample collection and ^{14}C analysis, respectively. NSF-OPP-ANT-0732467 also funded JAS to travel to Tulane University and analyze ramped pyrolysis samples using the PTP/CS and to travel to Woods Hole Oceanographic Institution to graphitize the samples. We thank 2 anonymous reviewers who improved the manuscript with their suggestions.

REFERENCES

Andrews JT, Domack EW, Cunningham WL, Leventer A, Licht KJ, Jull AJT, DeMaster DJ, Jennings AE. 1999. Problems and possible solutions concerning radiocarbon dating of surface marine sediments, Ross Sea, Antarctica. *Quaternary Research* 52(2):206–16.

DeMaster DJ, Ragueneau O, Nittrouer CA. 1996. Preservation efficiencies and accumulation rates for biogenic silica and organic C, N, and P in high-latitude sediments: the Ross Sea. *Journal of Geophysical Research* 101(C8):18,501–18.

Domack EW, Mashiotta TA, Burkley LA, Ishman SE. 1993. 300 year cyclicity in organic matter preservation in Antarctic fjord sediments. In: Kennett JP, Warnke DA, editors. *The Antarctic Paleoenvironment: A Perspective on Global Change (Part 2)*. Washington, DC: American Geophysical Union. p 265–72.

Domack EW, Ishman SE, Stein AB, McClennen CE, Jull AJT. 1995. Late Holocene advance of the Müller Ice Shelf, Antarctic Peninsula: sedimentological, geo-

https://doi.org/10.2458/azu_js_rc.v55i1.16234 Published online by Cambridge University Press

chemical and palaeontological evidence. *Antarctic Science* 7(2):159–70.

Domack EW, Leventer A, Dunbar RB, Taylor FW, Brachfeld S, Sjunneskog C, Party OLS. 2001. Chronology of the Palmer Deep site, Antarctic Peninsula: a Holocene palaeoenvironmental reference for the circum-Antarctic. *The Holocene* 11(1):1–9.

Domack EW, Duran D, Leventer A, Ishman S, Doane S, McCallum S, Amblas D, Ring J, Gilbert R, Prentice M. 2005. Stability of the Larsen B ice shelf on the Antarctic Peninsula during the Holocene epoch. *Nature* 436(7501):681–5.

Domack EW, Amblàs D, Gilbert R, Brachfeld S, Camerlenghi A, Rebesco M, Canals M, Urgeles R. 2006. Subglacial morphology and glacial evolution of the Palmer deep outlet system, Antarctic Peninsula. *Geomorphology* 75(1–2):125–42.

Licht KJ, Cunningham WL, Andrews JT, Domack EW, Jennings AE. 1998. Establishing chronologies from acid-insoluble organic ^{14}C dates on Antarctic (Ross Sea) and Arctic (North Atlantic) marine sediments. *Polar Research* 17(2):203–16.

Mackintosh A, Golledge N, Domack EW, Dunbar RB, Leventer A, White D, Pollard D, DeConto R, Fink D, Zhwartz D, Gore D, Lavoie C. 2011. Retreat of the East Antarctic ice sheet during the last glacial termination. *Nature Geoscience* 4(3):195–202.

McGeehin J, Burr GS, Jull AJT, Reines D, Gosse J, Davis PT, Muhs D, Southon J. 2001. Stepped-combustion ^{14}C dating of sediment: a comparison with established techniques. *Radiocarbon* 43(2A):255–61.

McGeehin J, Burr GS, Hodgins G, Bennett SJ, Robbins JA, Morehead N, Markewich H. 2004. Stepped-combustion ^{14}C dating of bomb carbon in lake sediment. *Radiocarbon* 46(2):893–900.

Michalchuk BR, Anderson JB, Wellner JS, Manley PL, Majewski W, Bohaty SM. 2009. Holocene climate and glacial history of the northeaster Antarctic Peninsula: the marine sedimentary record from a long SHALDRIL core. *Quaternary Science Reviews* 28(27–28): 3049–65.

Milliken KT, Anderson JB, Wellner JS, Bohaty SM, Manley PL. 2009. High-resolution Holocene climate record from Maxwell Bay, South Shetland Islands, Antarctica. *Geological Society of America Bulletin* 121(11–12):1711–25.

Mosola AB, Anderson JB. 2006. Expansion and rapid retreat of the West Antarctic Ice Sheet in eastern Ross Sea: possible consequence of over-extended ice streams? *Quaternary Science Reviews* 25(17–18): 2177–96.

Pudsey CJ, Barker PF, Larter RD. 1994. Ice sheet retreat from the Antarctic Peninsula shelf. *Continental Shelf Research* 14:1647–75.

Rosenheim BE, Day MB, Domack EW, Schrum H, Benthien A, Hayes JM. 2008. Antarctic sediment chronology by programmed-temperature pyrolysis; methodology and data treatment. *Geochemistry, Geophysics, Geosystems* 9(4):Q04005, doi: 10.1029/2007GC001816

Shevenell AE, Domack EW, Kernan GM. 1996. Record of Holocene paleoclimate change along the Antarctic Peninsula: evidence from glacial marine sediments, Lallemand Fjord. In: Banks MR, Brown MJ, editors. *The Climate of the Southern Ocean*. Hobart: Royal Society of Tasmania. p 55–64.

Shevenell AE, Ingalls AE, Domack EW, Kelly C. 2011. Holocene Southern Ocean surface temperature variability west of the Antarctic Peninsula. *Nature* 470(7333):250–4.

Stuiver M, Polach HA. 1977. Discussion: reporting of ^{14}C data. *Radiocarbon* 19(3)355–63.

van Beek P, Reyss J-L, Paterne M, Gersonde R, Rutgers van der Loeff M, Kuhn G. 2002. ^{226}Ra in barite: absolute dating of Holocene Southern Ocean sediments and reconstruction of sea-surface reservoir ages. *Geology* 30(8):731–4.

Wang H, Hackley KC, Panno SV, Coleman DD, Liu JCL, Brown J. 2003. Pyrolysis-combustion ^{14}C dating of soil organic matter. *Quaternary Research* 60(3):348–55.

Weber ME, Clark PU, Ricken W, Mitrovica JX, Hostetler SW, Kuhn G. 2011. Interhemispheric ice-sheet synchronicity during the Last Glacial Maximum. *Science* 334(6060):1265–9.

https://doi.org/10.2458/azu_js_rc.v55i1.16234 Published online by Cambridge University Press